Single-Domain Protein A-Engineered Magnetic Nanoparticles: Toward a Universal Strategy to Site-Specific Labeling of Antibodies for Targeted Detection of Tumor Cells

Serena Mazzucchelli,[†,‡,¶] Miriam Colombo,[†,‡,¶] Clara De Palma,[†] Agnese Salvadè,[†,‡] Paolo Verderio,[†,‡] Maria D. Coghi,[‡] Emilio Clementi,[†,§] Paolo Tortora,[‡] Fabio Corsi,[†] and Davide Prosperi[‡,⊥,*]

[†]Dipartimento di Scienze Cliniche "Luigi Sacco", Università di Milano, Ospedale L. Sacco, via G.B. Grassi 74, 20157 Milano, Italy, [‡]Dipartimento di Biotecnologie e Bioscienze, Università di Milano-Bicocca, piazza della Scienza 2, 20126 Milano, Italy, [§]Istituto Scientifico Eugenio Medea, 23842 Bosisio Parini, Italy, and [⊥]Istituto di Scienze e Tecnologie Molecolari, CNR, via Fantoli 16/15, 20138 Milano, Italy. [¶]These authors contributed equally to the research.

ABSTRACT Highly monodisperse magnetite nanocrystals (MNC) were synthesized in organic media and transferred to the water phase by ultrasound-assisted ligand exchange with an iminodiacetic phosphonate. The resulting biocompatible magnetic nanoparticles were characterized by transmission electron microscopy, dynamic light scattering, and magnetorelaxometry, indicating that this method allowed us to obtain stable particle dispersions with narrow size distribution and unusually high magnetic resonance T_2 contrast power. These nanoparticles were conjugated to a newly designed recombinant monodomain protein A variant, which exhibited a convincingly strong affinity for human and rabbit IgG molecules. Owing to the nature of antibody-protein A binding, tight antibody immobilization occurred through the Fc fragment thus taking full advantage of the targeting potential of bound IgGs. If necessary, monoclonal antibodies could be removed under controlled conditions regenerating the original IgG-conjugatable MNC. As a proof of concept of the utility of our paramagnetic labeling system of human IgGs for biomedical applications, anti-HER-2 monoclonal antibody trastuzumab was immobilized on hybrid MNC (TMNC). TMNC were assessed by immunoprecipitation assay and confocal microscopy effected on HER-2-overexpressing MCF-7 breast cancer cells, demonstrating excellent recognition capability and selectivity for the target membrane receptor.

KEYWORDS: magnetic nanoparticles · targeted MRI contrast agents · phase transfer · biolabeling · protein A · breast cancer

Noninvasive medical imaging methods currently represent a major issue in the prevention and treatment of malignant diseases.[1] Among them, magnetic resonance imaging (MRI) is rapidly becoming the gold-standard technique for an in-depth tissue investigation with high-spatial resolution.[2,3] However, in several circumstances, MRI suffers from low sensitivity, which is critical when accurate detection and monitoring of localized malignancies developing in the early stages of the disease are required. For this reason, great efforts have been made to develop efficient contrast enhancing agents aimed at improving the signal difference between the area of interest (*e.g.*, the blood pool) and the background. In clinical application, the systemic injection of appropriate doses of contrast agents, mostly based on gadolinium complexes (*e.g.*, Gd-DTPA),[4,5] results in a nonspecific enhancement of the MRI signal. When a sharp tissue distribution is desired, targeted contrast agents are designed in such a way that they localize to specific cell type through active binding mechanisms, which exploit the conjugation of the signal enhancer with suitable markers. Among them, most used are folate, small peptides, and antibodies, which stimulate specific recognition with the respective tumor cell receptor.[6−8] Unfortunately, in most cases, antibody-conjugated Gd-DTPA proved to be largely unsuccessful due to the relatively low sensitivity of MRI and the low density of cell target receptors, thus requiring administration of excessive gadolinium doses. This drawback can be partially overcome by using magnetic nanoparticles based on iron oxide (MNPs), which have been demonstrated to induce large increments in transverse relaxation rate upon binding with a 10^6 signal amplification over Gd-DTPA.[9] While Gd-based agents enhance the signal in T_1-weighted images, MNPs provide strong signal enhancement in T_2-weighted images, owing to a different contrasting mechanism.[10,11] For this reason, MNPs have attracted much attention in biomedical diagnostics in view of their usefulness as contrast agents for magnetic

*Address correspondence to davide.prosperi@unimib.it.

Received for review June 10, 2010 and accepted August 31, 2010.

Published online September 8, 2010.
10.1021/nn101307r

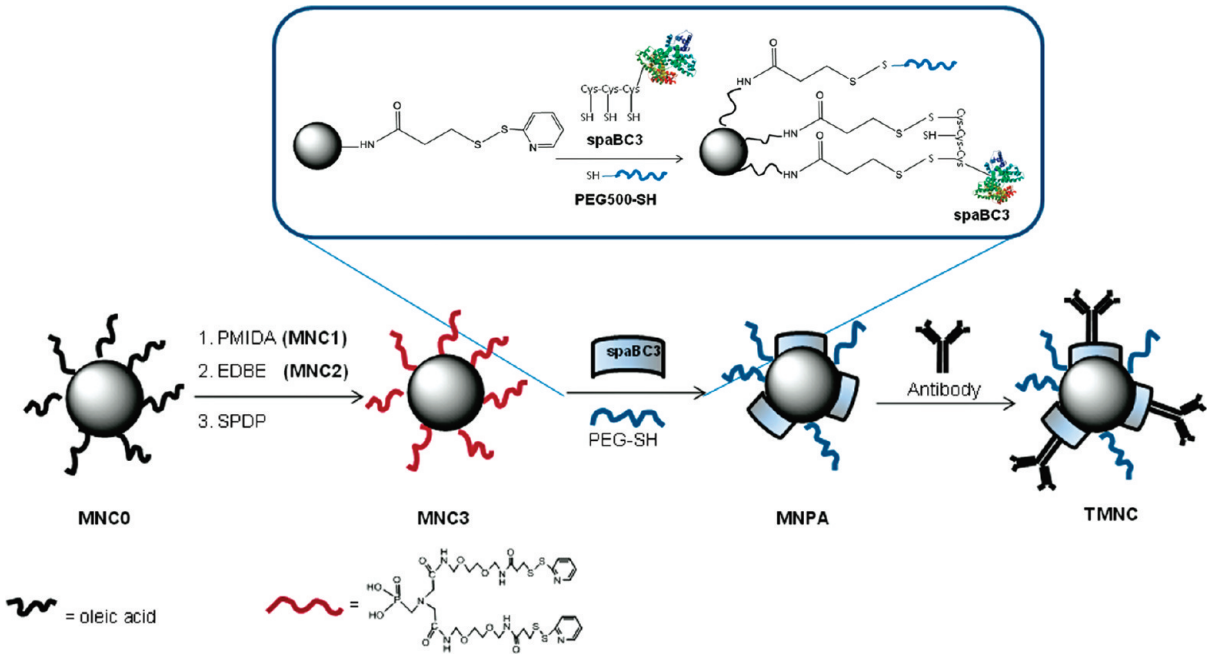

Scheme 1. Synthesis of Pegylated Trastuzumab-Functionalized MNC (TMNC)

resonance imaging (MRI)[12−14] and biosensing.[15] Moreover, the hydroxyl-rich surface of iron oxides promotes the direct conjugation of organic and biological molecules by surface chemical technology.[16] The design and construction of a successful target-oriented biohybrid paramagnetic nanoprobe is a primary goal toward the development of highly efficient contrast enhancer for MRI, standing at the interface between nanotechnology and molecular biology. The ultimate challenge is represented by the development of reliable strategies for the conjugation of targeting biomolecules, especially monoclonal antibodies (IgGs), to MNPs. These include passive/electrostatic physical adsorption of IgGs, tight immobilization exploiting the strong interaction of biological counterparts, such as biotin-streptavidin, which requires prior IgG biotinylation,[17] or the formation of covalent chemical connections, which is often considered the most practical choice.[18,19] Although these approaches may offer different solutions and have been successfully employed in several circumstances, they all share the same basic limitation, that is a non-site-specific binding to IgG molecule, which affects the targeting efficiency of the antibody. As a matter of fact, the actual conservation of the targeting bioactivity of immobilized IgGs is not obvious and remains a crucial issue, which must be addressed in designing a successful targeted nanoprobe.

An interesting option might be envisaged in the use of a natural peptide linker endowed with high affinity for IgGs, such as protein A. Protein A is a cell-wall associated protein exposed on the surface of the gram-positive bacterium *Staphilococcus aureus*.[20] The primary structure consists of a 42 kDa single polypeptide chain, folded into five highly homologous domains, named E, D, A, B, and C, each consisting of 56−61 residues.[21] The interest for this molecule in biotechnology resides mainly in three useful properties: (1) the protein structure is stable over a broad range of pH (2−12) and in the presence of various detergents; (2) it can bind reversibly a large variety of IgGs *via* their Fc fragment through its consensus sequence (Asn-Gln-Phe-Asn-Lys-Glu),[21] (3) IgG-protein A complex can be dissociated under controlled conditions (pH 3.5−4.5) without apparent loss of activity.[22] The affinity of protein A for immunoglobulins is not conserved among the different classes and isotypes. In particular, it exhibits high affinity to human, rabbit, and guinea pig IgGs. Recently, natural protein A has been used immobilized on magnetic polyadsorbent for IgG separation and/or purification procedures.[23] As protein A recognizes the Fc portion of IgGs, it is expected to mediate an orderly Fc site-specific antibody immobilization on MNPs resulting in a target-directed Fab presentation.[24]

In this paper, we present a multidisciplinary approach to the design and synthesis of a universal magnetic nanohybrid consisting of a high-quality iron oxide nanocrystal core conjugated to a suitably bioengineered small variant of protein A for the smart immobilization of IgGs. The resultant targeted nanoparticle is shown to exhibit high affinity and selectivity for the appropriate tumor markers. As a case study for our investigations, we focused on the monoclonal antibody trastuzumab, which is commonly employed in clinical therapy of breast cancer, as a model for the development of our tumor-targeting magnetic nanoprobe. Trastuzumab (tz) is a humanized monoclonal antibody consisting of two antigen-specific sites that bind to the juxtamembrane portion of the extracellular domain of

the "Human Epidermal growth factor Receptor 2" (HER-2), which is found overexpressed in several metastasizing breast cancer cells.[25]

RESULTS AND DISCUSSION

Our aim was to synthesize a model magnetic nanoparticle hybrid system containing a specific IgG binding functionality with the lowest molecular weight to reduce the nanoparticle overall size. We reasoned that a recombinant derivative of protein A consisting of one single IgG-binding domain, namely the B domain, would meet such criteria. This strategy displays several advantages: (1) as for entire protein A, all the antibodies are presented in the same orientation on the nanoparticle, with the active Fab portions directed in an optimal configuration for antigen binding; (2) the use of a single B domain of protein A results in a very small biomolecular support for the antibody, which is expected to partially reduce the immunogenicity of the whole hybrid nanoparticle, while conserving remarkable binding affinity for IgGs; (3) the bioengineering approach to the protein A variant allows for the artificial introduction of selectively reactive functionalities in the peptide sequence, such as cysteine thiols, for site-specific conjugation onto the nanoparticle surface. The promising combination of all these potential advantages prompted us to explore the possibility of improving the current methods for the synthesis of IgG-functionalized nanohybrids. We chose an organic-phase approach for the synthesis of the magnetite core nanostructure, providing highly uniform and crystalline magnetic nanoparticles endowed with strong intrinsic relaxivity and narrow size distribution. This approach, while effective, had a main limitation, which was the poor solubility of the resulting surfactant-coated nanoparticles. Hence, an efficient ligand exchange was required to transfer them into an aqueous environment avoiding particle aggregation. Scheme 1 depicts the general strategy followed to synthesize tz-functionalized magnetic nanocrystals (TMNC), which were then assessed according to their capability to recognize the HER-2 receptor antigen both in a whole cell extract and in living cultured breast cancer cells.

Development of Water-Stable Profunctional Iron Oxide Nanocrystals. High-quality, 8 nm hydrophobic iron oxide nanocrystals (MNC0, Figure 1, inset) were synthesized by solvothermal decomposition from iron−oleate complex in a solution of octadecene in the presence of oleic acid as capping agent.[26] The synthesized uniform nanocrystals were finely dispersed in chloroform and treated under continuous sonication with an excess of *N*-phosphonomethyl iminodiacetic acid phosphonate (PMIDA) dissolved in aqueous ammonia solution to promote the ligand exchange on the MNC0 surface, leading to the highly water dispersible, readily functionalizable MNC1. The phase transfer reaction occurred quickly thanks to the higher affinity of PMIDA phosphonate group toward iron oxide compared to oleic carboxylate (Figure 1a, inset). After the phase transfer, MNC1 maintained the original average crystal size (8

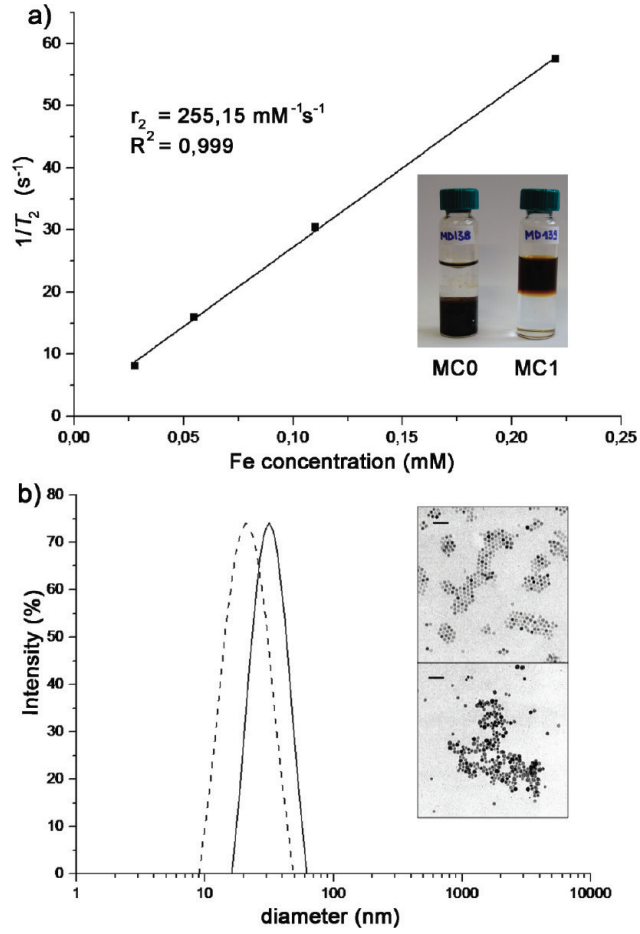

Figure 1. (a) T_2 relaxometry analysis of as-synthesized MNC1. The inverse of experimental T_2 values obtained at different MNC1 concentrations is plotted *vs* iron concentration. The experimental data are fitted by a line. The line slope indicates the T_2 relaxivity. Inset: MNC phase transfer from organic solvent (chloroform) to aqueous solution. (b) Hydrodynamic size distribution histograms of oleic-coated Fe_3O_4 nanoparticles (dashed line) and after ligand exchange with PMIDA (MNC1, continuous line). Diameters were measured by DLS in chloroform and water, respectively. Inset: TEM images of as-synthesized MNC0 in hexane (top) and of MNC1 in PBS (bottom). Scale bars = 50 nm.

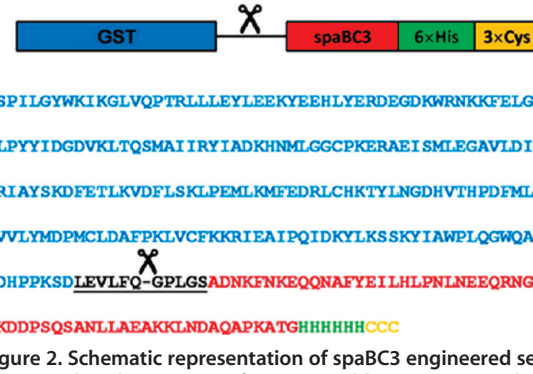

Figure 2. Schematic representation of spaBC3 engineered sequence. Glutathione *S*-transferase (GST, blue), spaBC3 (red), histidine tag (green), and cysteine tripod (orange). PreScission protease cleavage site between amino acids Gln_{226} and Gly_{227} is evidenced.

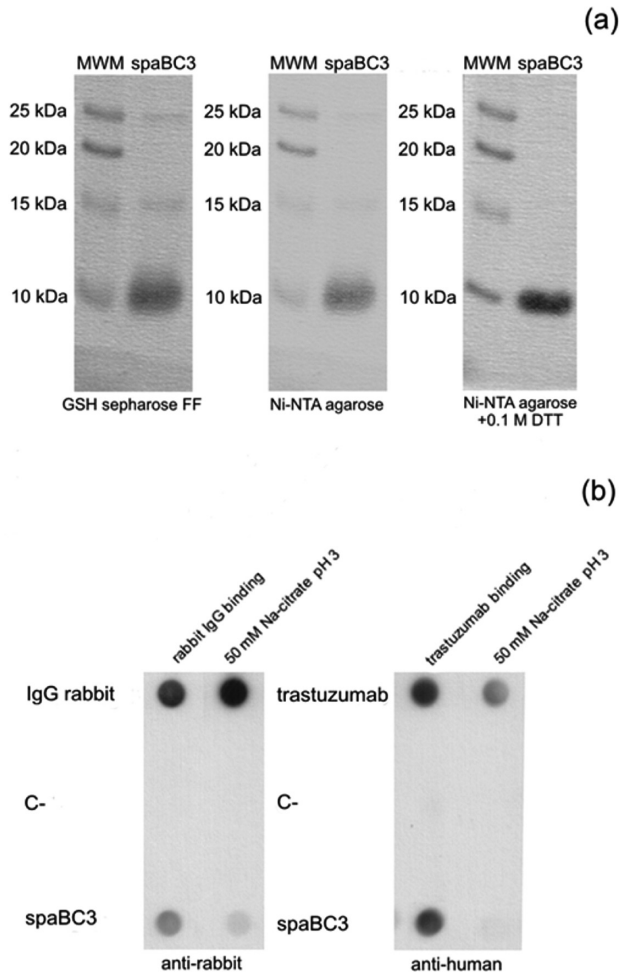

Figure 3. (a) SDS-PAGE of spaBC3 purified fractions. Molecular weight markers (MWM, 5 μL) Precision Plus Unstained were used. Purified protein (4 μg) was loaded after elution with PreScission protease (left). After purification with Ni-NTA agarose to remove GST contaminants, the same amount of spaBC3 was loaded on SDS-PAGE with or without 0.1 M DTT in running buffer (right and middle, respectively). (b) SpaBC3 binding assay. SpaBC3 (250 ng) was filtered through PVDF membrane and incubated with rabbit IgG or tz. IgG removal was obtained by Na-citrate incubation. GST protein (C-, 250 ng), as negative control, and rabbit IgG or tz (250 ng), as positives, were used. The presence of rabbit IgG or tz was revealed by antirabbit or antihuman secondary antibodies conjugated to HRP, respectively.

nm, by TEM), the final nanoparticle shape was uniformly spherical, while a slight increase in the hydrodynamic diameter from 21 ± 2 nm (MNC0 in chloroform) to 32 ± 3 nm (MNC1 in water) was determined by dynamic light scattering (DLS) (Figure 1b), probably due to the change of solvent and solvation aptitude of the new ligands. The resulting MNC1 surface, rich of accessible carboxyl groups, stabilized well the colloidal particles in buffered solution by electrostatic repulsions, concomitantly providing a useful support for further functionalization. In addition, we performed relaxometric measurements to determine the T_2 enhancing capability of synthesized nanocrystals. The water-soluble MNC1 exhibited a remarkably high transverse relaxivity ($r_2 = 255\ mM^{-1}\ s^{-1}$ at 20 mHz, $\mathbf{B}_0 = 0.47$ T), deduced by the slope of the line obtained by plotting $1/T_2$ *vs* iron concentration. This value, as compared with the relaxivity of commercially available T_2 contrast agents based on polymer-coated iron oxides, such as Endorem (Guerbet, 160 $mM^{-1}\ s^{-1}$), Ferumoxytol (Adv. Magnetics, 83 $mM^{-1}\ s^{-1}$), and Resovist (Schering, 151 $mM^{-1}\ s^{-1}$), suggests that high contrast power can be achieved with MNC1, on the same order of the best T_2 contrast agents reported so far.[27]

Carboxylate functionalities were converted into amine ends by reaction with the bifunctional diamino-linker 2,2-(ethylenedioxy)bis(ethylamine) (EDBE) *via* *N*-hydroxysuccinimidyl ester (NHS) activation. EDBE-modified nanoparticles (MNC2) exhibited a hydrodynamic diameter of 57 ± 3 nm, as determined by DLS. The average number of amino groups on MNC2 was quantified by an adapted version of the Dunnill's protocol,[28] resulting in 150 amines per particle. Our two-step procedure involving hot organic synthesis of monocrystalline iron oxide followed by ligand exchange and phase transfer allowed us to obtain stable water-soluble nanoparticles with unique contrast power and narrow size distribution, typical of the thermal synthesis in high-boiling organic solvent, yet devoid of the drawbacks associated to the biological fluid incompatibility. The high relaxivity value of our soluble MNC makes this nanoprobe a promising contrast agent applicable in magnetic resonance imaging (MRI) for the potential noninvasive diagnosis of malignances.

MNC2 were stable for months with nondetectable precipitation in several buffered media, including Dulbecco's PBS, pH 7.4; borate buffer, pH 8.5; acetate buffer, pH 5.0; and tris HCl, pH 6−8. The amino functionalities on the particle surface allowed the MNC2 conjugation with *N*-succinimidyl-3-[2-pyridyldithio]-propionate (SPDP) *via* NHS ester resulting in the thiol-reactive pro-functional MNC3 (Scheme 1). MNC3 were the ideal building block for bioconjugation with thiol-engineered protein A variant, as PDP functionality is unaffected by nucleophiles but very reactive toward sulfhydryl ends of organic and biological thiol-containing molecules under mild conditions by formation of stable disulfide bridges.

Design, Expression, and Purification of an Engineered Cys_3-Ended Variant of a Single-Domain Fragment of Protein A from *Staphylococcus aureus*. The B domain sequence, previously reported by Abrahmsen *et al.*,[21] was modified inserting *Bam*HI and *Sma*I restriction sites at the 5′ and 3′ positions, respectively. The modified gene was cloned to express the B domain in fusion with glutathione *S*-transferase (GST). However, proteins purified by GST affinity chromatography may contain small amounts of GST and GST-affine contaminants in eluted fractions. For this reason, a supplementary 6× His affinity tag was introduced at the C-terminal to completely remove the residual GST-deriving impurities through an additional affinity purification step.[29] To achieve a site-specific con-

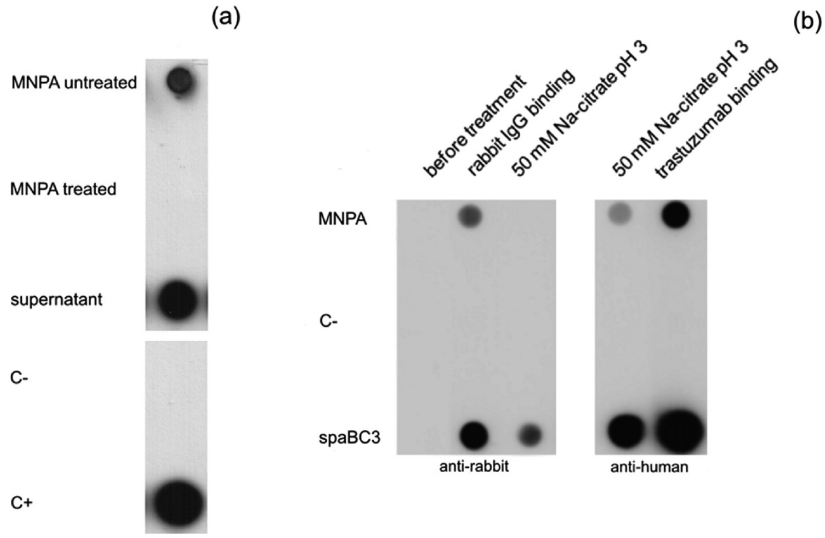

Figure 4. (a) Assessment of SpaBC3-MNC conjugation. MNPA was treated with 0.1 M DTT, resulting in spaBC3 release. The reduced MNPA was loaded on a PVDF membrane, together with untreated MNPA and the supernatant from the reduction mixture as controls. The presence of spaBC3 was detected by antihuman HRP-antibody only in untreated MNPA and in supernatant samples, confirming that SpaBC3 was anchored onto MNC essentially *via* disulfide bridges. C− and C+ are GST protein (250 ng) and spaBC3 (250 ng), respectively. (b) SpaBC3 on MNPA retains its IgG binding activity. MNPA (500 ng) was filtered through PVDF membrane and incubated with rabbit IgG or tz. IgG removal was obtained by Na-citrate incubation. GST protein (C−, 250 ng) and spaBC3 (C+, 250 ng) were used as negative and positive controls, respectively. MNPA capture of rabbit IgG or tz was revealed by antirabbit or antihuman secondary HRP-antibodies, respectively.

jugation of the protein A variant to MNC, the presence of one selectively reactive group in the protein primary structure was required. As the recombinant B domain was devoid of cysteine residues, we envisaged that the incorporation of a cysteine tail would result in the introduction of a highly reactive thiol group, concomitantly avoiding potentially competitive interferences from other functional moieties in the peptide sequence. In light of our preliminary results showing an unexpected weakness of the protein−nanoparticle linkage with one single Cys tagged behind the His_6 terminal (data not shown), we substituted the single Cys residue with a Cys_3 tripod leading to an improved binding effectiveness of the thiol end (Figure 2).

The engineered domain B of protein A from *Staphilococcus aureus* containing a C-terminal His_6Cys_3 tail (spaBC3) was cloned in fusion with GST tag in pGEX-6P-1 vector and expressed in BL21(DE3) *E. coli* strain. SpaBC3 was subsequently purified using a GST affinity column and eluted with cleavage with PreScission protease, obtaining a 7.48 kDa protein with a good degree of purity showing the presence of two residual contaminants at 15 and 25 kDa, respectively, which were removed by further purification through a Ni-NTA agarose column. SDS-PAGE performed under conventional reducing conditions showed a remarkably diffuse band at *ca.* 10 kDa in correspondence of spaBC3, suggesting that during acrylamide gel migration the formation of disulfide bridges between spaBC3 molecules leading to aggregates might occur. By addition of 0.1 M dithiothreitol (DTT) in the running buffer, a more defined thin spaBC3 band was obtained. These experiments are summarized in Figure 3a. While a DTT concentration of about 25 mM is usually estimated to be sufficient to break intermolecular monodentate disulfide bridges,[30] here the presence of a cysteine tripod forced us to use more strongly reducing conditions to maintain spaBC3 in its monomer form until its conjugation with nanoparticles.

SpaBC3 Retains IgG Binding Activity. Recombinant spaBC3 produced in *E. coli* and filtered on a polyvinylidene fluoride (PVDF) membrane was assessed in regard to its ability to bind IgG molecules. In Figure 3b, a dot blot example of spaBC3 complex incubated with rabbit IgG is presented. The presence of bound IgG was revealed by a strong signal of antirabbit secondary antibody conjugated with horseradish peroxidase (HRP). To evaluate the possibility to recycle spaBC3 for multiple usages, we tested the IgG removal by incubating the spaBC3-IgG complex in 50 mM Na-citrate buffer, pH 3 at room temperature (RT), observing a remarkable reduction of the signal from 30 min of treatment. The same spaBC3 sample was then incubated with a solution containing tz, confirming the ability of spaBC3 to capture different IgGs even after Na-citrate treatment. These results suggested to us that spaBC3 might be exploited for the pro-functionalization of nanoparticles leading to a universal nanocarrier for the efficient, recyclable, and target-directed conjugation of a large variety of IgGs.

Conjugation of spaBC3 to MNC through Sulfhydryl Groups. SpaBC3 was incubated in 0.1 M DTT to reduce the cysteine residues, and then the excess of DTT was removed by gel filtration. The purified monomer protein obtained by this procedure was immediately incubated with MNC3 and left overnight. Under these conditions, the thiol groups of cysteine residues displayed high re-

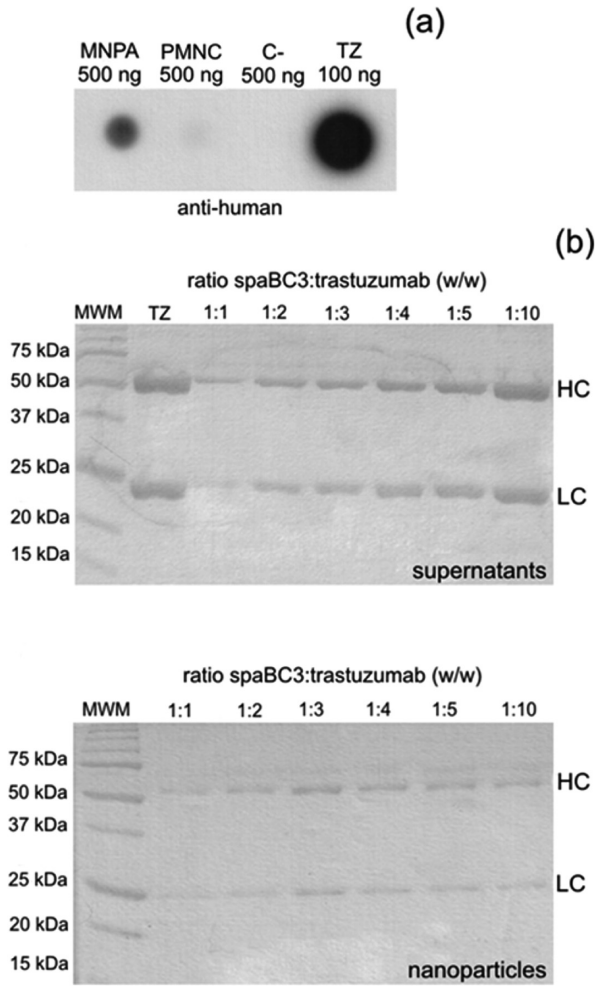

Figure 5. (a) Trastuzumab conjugation to MNPA. MNPA and PMNC incubated in parallel with an equal amount of tz for 1 h at 25 °C were filtered through a PVDF membrane. Tz and GST were used as positive and negative controls, respectively. Membrane dot blot was probed with antihuman HRP-antibodies and the immobilization of tz was revealed by an ECL detection system. (b) Coomassie-stained gels demonstrating the binding capability of MNPA. A fixed amount of MNPA was mixed with increasing amounts of tz and precipitated after 1 h incubation. Supernatants and resuspended pellets were analyzed by SDS-PAGE using tz as control. HC, IgG heavy chain; LC, IgG light chain; MWM, molecular weight marker Precision Plus Unstained.

activity and reacted rapidly with PDP functionalities on MNC3, which could be monitored by UV detection at 343 nm of the released pyridine-2-thione.[31] Notably, given the reactivity of the Cys_3 tripod, we noticed that it is of primary importance that reduced spaBC3 is incubated with MNC3 immediately after DTT treatment to obtain a satisfactory extent of conjugation. Next, we determined the amount of spaBC3 immobilized on MNC by Bradford assay of the supernatant and found that 1 mg of MNC3 was able to bind 167 μg of protein. The residual PDP functionalities on spaBC3-MNC were reacted with an excess of PEG_{500}-SH to saturate the reactive groups on the nanoparticles thus minimizing the possibility of accidental interaction with nonspecific proteins.

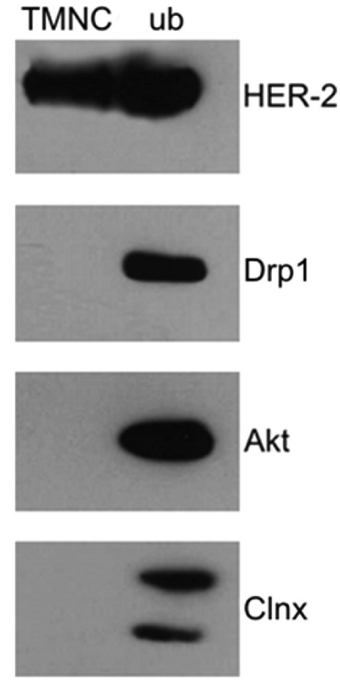

Figure 6. HER-2 receptor is selectively recognized by TMNC. Immunoprecipitation was performed using 200 μg of TMNC. Nanoparticles were incubated overnight at 4 °C with 1 mg protein in a whole extract of MCF-7 cells. Bound and unbound proteins were then eluted in SDS-PAGE application buffer, electrophoresed, and immunoblotted using either anti-HER-2, anti-Drp1, anti-Akt, and anti-Clnx antibodies.

To prove that spaBC3 was actually anchored to the MNC surface through disulfide bridges, the spaBC3-MNC conjugate (MNPA) was treated with 0.1 M DTT, which was expected to break the disulfide bridges leading to spaBC3 release. On the contrary, in case spaBC3 was captured by MNC through nonspecific physical adsorption, the protein should at least partially remain anchored to the MNC surface after DTT treatment, as the reducing environment would not affect its surface adhesion. Hence, the reduced MNPA was loaded on a PVDF membrane, together with untreated MNPA and the supernatant from the disulfide bridges reduction mixture as controls (Figure 4a). The signal of spaBC3 was indeed recovered only in untreated MNPA and in supernatant samples. This result clearly demonstrates that spaBC3 was bound to MNC exploiting the tripod tail selectively *via* disulfide bridge formation without aspecific adsorption.

Eventually, we evaluated the capability of MNPA to retain the ability to capture an IgG molecule and be reutilized to bind different monoclonal antibodies after Na-citrate treatment. MNPA, free spaBC3, and a protein used as negative control, namely GST, were individually filtered through a PVDF membrane. Each sample was incubated with rabbit IgG, then treated with Na-citrate buffer, and finally incubated with tz. Figure 4b clearly shows that both the IgG binding experiments performed with MNPA and their recycle after Na-citrate treatment were successful. We concluded that MNPA

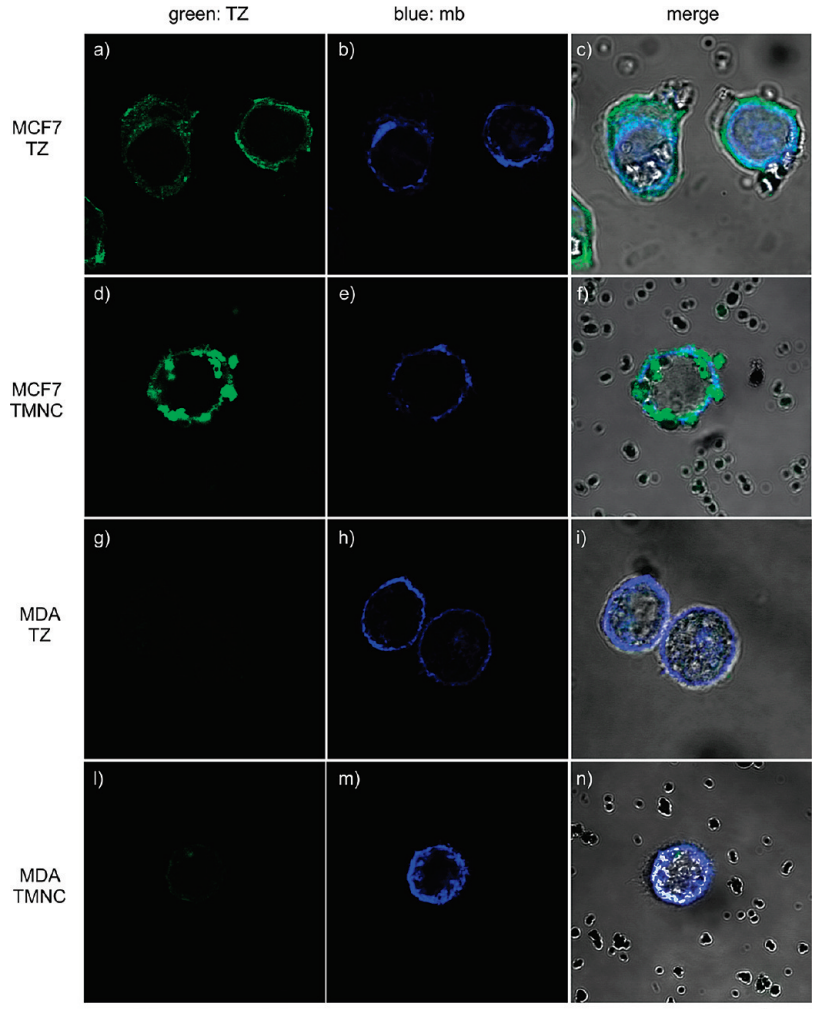

Figure 7. Confocal laser images of MCF-7 and MDA cells cultured with TMNC or free tz. MCF-7 and MDA were incubated for 15 min with TMNC (150 μg mL^{-1}; panels d−f and l−n, respectively) and tz (15 μg mL^{-1}; panels a−c and g−i, respectively). Cell membranes (mb) were stained with DiD oil (blue). TMNC and tz were labeled with antihuman FITC secondary antibodies. Scale bar =10 μm.

is a good candidate to be developed as a universal magnetic nanoparticle model system useful for the reliable and straightforward conjugation of human(ized) antibodies.

Trastuzumab Immobilization on MNPA. MNPA and fully pegylated MNC devoid of spaBC3 (PMNC, control) were incubated in parallel with an equal amount of tz. Trastuzumab conjugation was assessed in each sample by filtering the respective solutions through a PVDF membrane, which was subsequently probed with antihuman antibodies conjugated to HRP. Trastuzumab and GST were used as positive and negative controls, respectively. Dot blot assay was positive only with MNPA, which confirmed the occurred immobilization of tz through spaBC3 specific interaction (Figure 5a). Next, we optimized the antibody/MNPA ratio to maximize the number of tz molecules bound to MNPA while maintaining the minimal excess in the supernatant. This is important because our results showed that it was not possible to saturate the whole spaBC3 supported on MNC. MNPA was incubated with increasing amounts of tz. Coomassie stain of both supernatant and nanoparticles used in the conjugation reaction evidenced that the best results were obtained incubating MNPA in a spaBC3/tz ratio of 1:3. The comparison between upper and lower gels in Figure 5b evidence that, above the 1:3 ratio, the amount of loaded antibody did not increase, while a remarkable progressive increment of IgG concentration in the supernatant was observed. Under the above conditions, we determined that the tz-functionalized MNC (TMNC) displayed an average of 1.8 IgG molecules per MNC, corresponding to *ca.* 0.1 mg tz per mg MNC.

TMNC Display Binding Capability to HER-2 Receptor. MCF-7 whole cell extracts were incubated overnight at 4 °C on a rotating wheel with TMNC. TMNC and the supernatant (unbound, ub) were analyzed by Western blotting with anti-HER-2 antibody in order to reveal HER-2 binding to TMNC (Figure 6). Our data confirmed that TMNC were able to immunoprecipitate HER-2 membrane receptor in a whole cell extract. This immunoprecipitation was highly specific, as antibodies recognizing dynamin-

related protein (Drp1) and Akt, two soluble cytosolic proteins, or calnexin (Clnx), an integral protein of the endoplasmic reticulum, which were tested as negative controls, displayed a detectable signal only in the ub sample. These results indicate that Clnx was absent in the TMNC sample, whereas it was detected in the unbound, suggesting that the interaction between TMNC and HER-2 is specific and related to antibody conjugation. This clearly highlights the remarkable target-selectivity of TMNC toward the HER-2 breast cancer cell marker.

To validate the immunoprecipitation data, the specificity of binding between TMNC and HER-2 was observed by confocal laser scanning microscopy. Indeed, as HER-2 is a trans-membrane receptor, TMNC were expected to accumulate in correspondence of the external surface of HER-2-overexpressing cells. This should allow us to discriminate between receptor-mediated particle capture by cell membrane and residual unspecific uptake promoted by alternative pathways.[32] HER-2 positive MCF-7 cells[33] (Figure 7a−c) and, as a negative control, HER-2 negative MDA cells (Figure 7g−i) were treated with tz in order to assess HER-2 expression and cellular surface distribution. TMNC were incubated in parallel with both MCF-7 and MDA cells at a concentration of 150 μg mL^{-1} culture medium. Trastuzumab and TMNC were labeled with antihuman FITC-labeled secondary antibodies (green), whereas cell membranes were stained with DiD oil (mb, blue). As expected, after 15 min incubation, TMNC were observed in HER-2 positive MCF-7 cell surfaces (Figure 7d−f), but not in MDA negative control cells (Figure 7l−n), demonstrating that they localized selectively in correspondence of trans-membrane receptors owing to the presence of the specific targeting agent.

CONCLUSIONS

High-quality biocompatible magnetite nanocrystals (MNC) were obtained by phase transfer of oleate-coated iron oxides *via* successful ligand exchange with an iminodiacetic acid phosphonate exploiting the strong affinity of phosphonate for iron oxide. Such water-soluble nanocrystals exhibited a transverse relaxation rate of 255 mM^{-1} s^{-1}, which is significantly higher than commercially available T_2 contrast agents based on polymer-coated iron oxides. A recombinant low-molecular-weight fragment of protein A modified to present a terminal cysteine tripod was synthesized, characterized, and conjugated to MNPs through an appropriate bifunctional linker affording a molecular nanohybrid suitable for site-specific immobilization of antibodies. The antibody capture capacity of our hybrid nanoparticles was successfully tested with trastuzumab and rabbit IgGs. In particular, trastuzumab-conjugated MNC were effective in selectively recognizing HER-2 receptor expressed in MCF-7 breast cancer cells. The model nanoparticle system (MNPA) presented here enables efficient and reversible labeling of a large variety of human monoclonal antibodies with highly conserved biological activity toward their natural receptors. The combination of all these properties renders our newly developed MNPA a promising versatile nanoscale probe for application in targeted diagnosis of tumor cells and tissues.

EXPERIMENTAL SECTION

Synthesis of MNC3. All reagents and solvents were analytical grade (Sigma-Aldrich, St. Louis, MO). MNC0 were synthesized according to Park *et al.*[26] TEM images of the nanoparticles were obtained by a Zeiss EM-109 microscope (Oberkhochen, Germany) operating at 80 kV. Hydrodynamic diameters were obtained by DLS measurements performed at 90° with a 90Plus Particle Size Analyzer working at 15 mW of a 661 nm solid state laser (Brookheaven Inst., Holtsville, NY). Surface ligand exchange was performed as follows. Dried MNC0 (40 mg) were dispersed in chloroform (4 mL). A 0.1 M PMIDA solution was prepared dissolving PMIDA (345 mg) in diluted ammonium hydroxide (28%, 4.5 mL in 11.5 mL water) and added to the above MNC0 dispersion. The mixture was sonicated and sporadically stirred for 30 min without capping the reaction flask, so to encourage the evaporation of the organic solvent. The PMIDA-coated particles (MNC1) were then recovered by magnetic decantation, washed once with 10 mL of the above 0.1 M PMIDA solution, and separated again by permanent magnet. Particles were washed several times with water until pH was neutral and precipitated by the addition of a mixture of acetone/ethanol. Next, a concentrated solution of MNC1 was dialyzed in deionized water and finally diluted to a concentration of 1 mg mL^{-1}. Relaxation measurements were performed at a temperature of 313 K on a Bruker Minispec mq20 system (Ettlingen, Germany) working with ^1H at 20 MHz magnetic field with the following parameters: CMPG pulse sequence, 1000 echoes with a 20 ms echo time and 2 s repetition time. NHS (15.4 mg) and EDC (11.2 mg) were added to 7 mL of the above MNC1 solution, followed by 0.5 M NaOH until pH 8 (*ca.* 2.6 mL). EDBE (196 μL) was then added and the reaction was left under stirring overnight. Excess EDBE was removed by dialysis obtaining MNC2, and the amount of amine groups was quantified by Dunnill's protocol.[28] MNC2 (10 mg) were suspended in a mixture of dry DMF (1.6 mL) and DMSO (0.4 mL) under Ar and sonicated 15 min to obtain a proper dispersion. SPDP[34] (3 mg) dissolved in dry DMSO (0.5 mL) and diisopropylethylamine (1 μL) were consecutively added under stirring. The reaction was quenched after 15 h adding acetic acid (1 μL). Particles (MNC3) were recovered by centrifugation and washed with water until neutral pH and finally exsiccated under vacuum, ready for the next conjugation steps.

DNA Synthesis and Cloning in pGEX-6P-1 Vector. A modified DNA sequence encoding for domain B of *Staphilococcus aureus* protein A was synthesized (Eurofins MWG Operon, Ebersberg) to obtain a fragment variant containing a 6 × His C-terminal tail and *Bam*HI and *Sma*I restriction sites, respectively, at 5′ and 3′ positions (SpaB). SpaB DNA sequence was cloned in a pGEX-6P-1 vector (GE Healthcare, Life Sciences, Little Chalfont, UK) between *Bam*HI and *Sma*I restriction sites according to the Molecular Cloning Handbook,[35] to obtain spaB as a GST-fusion protein containing a PreScission protease recognition site. Plasmidic DNA was then mutated using Quick Site-change mutagenesis kit (Stratagene, La Jolla, CA) in order to introduce a cysteine tripod at C-terminal. The following mutagenesis primers were used: 5′-Cys-5′-CCGGTCACCACCATTGCTGCTGTTAACCCGGGTCGAC-3′ and 3′-Cys-5′-GTCGACCCGGGTTAACAGCAGCAA-TGGTGGTGACCGG-3′. Plasmidic DNA obtained by this procedure (pGEX/spaBC3) was sequenced and used to transform *E.*

coli expression strain BL21(DE3)-RIL (*E. coli* B F$^-$ *ompT hsdS* (rB$^-$ mB$^-$) *dcm*$^+$ *gal*λ(DE3) (Stratagene).

SpaBC3 Expression and Purification. *E. coli* strain BL21(DE3)-RIL expressing spaBC3 as GST-fusion protein were grown at 37 °C in LB-ampicillin medium and induced with 0.5 mM IPTG at A_{600} 0.8 for 3 h. Cells of mass 1.5 g were obtained from 500 mL of culture. To prepare crude extract, cells were resuspended in lysis buffer (5 mL g^{-1} wet weight; 25 mM potassium phosphate, pH 7.2, 150 mM NaCl, 0.5 mM phenylmethanesulfonyl fluoride, 5 mM DTT, 100 mM $MgCl_2$) plus 1 mg mL^{-1} lysozyme and incubated for 1 h at 4 °C. The cell suspension was then frozen at −80 °C for 30 min and thawed, DNaseI (0.2 mg g^{-1} cells, wet weight) and 1% Triton X-100 were added, and the sample was further incubated for 30 min at RT. Finally, it was centrifuged for 30 min at 39000*g*. Supernatant was loaded onto Glutathione Sepharose 4B affinity column (0.5 mL bed volume, GE Healthcare). Then, it was washed with 20 volumes of washing buffer (25 mM potassium phosphate, pH 7.2, 150 mM NaCl) and equilibrated with 10 volumes of cold cleavage buffer (50 mM Tris-HCl, pH 7.0, 150 mM NaCl, 1 mM EDTA, 1 mM DTT). To elute spaBC3, the resin was incubated at 4 °C overnight under shaking with Prescission protease (400 U mL^{-1} resin) (GE Healthcare). Protein eluted with PreScission protease cleavage was then loaded onto Ni-NTA affinity column (0.5 mL bed volume) and washed with 50 mM sodium phosphate, pH 8.0, 0.3 M NaCl, 20 mM imidazole. SpaBC3 was eluted with 50 mM sodium phosphate, pH 8.0, 0.3 M NaCl, 0.5 M imidazole. Protein was assayed using the reagent Coomassie brilliant blue G-250 (Pierce Biotechnology, Rockford, IL), using bovine serum albumin (BSA) as standard protein.

SDS-PAGE and spaBC3 Binding Assay Using Dot Blot. SDS-PAGE[36] was carried out in a Mighty Small apparatus (Hoefer Scientific Instruments, San Francisco, CA) with a 15% running gel and a 4% stacking gel, 2 h at 25 mA. An aliquot of 0.1 M DTT was added to running buffer. Proteins were revealed by gel code staining (Pierce Biotechnology). Dot blot was performed by filtering proteins and/or nanoparticles onto PVDF membranes, utilizing a Minifold I dot blot apparatus (GE Healthcare), and incubating in blocking solution (5% skim milk in PBS) for 1 h at RT. To evaluate spaBC3 activity, membranes were then probed for 1 h at 25 °C using rabbit IgG (1 mg mL^{-1}) at a 1:800 dilution, or tz (1 mg mL^{-1}) at a 1:6000 diluition in PBS buffer, respectively. Membranes were rinsed three times in 0.05% Tween in PBS for 10 min each and subsequently incubated for 1 h at RT with a secondary antibody (1:5000 horseradish peroxidase−goat antirabbit antibodies in 0.05% Tween in PBS or 1:20000 horseradish peroxidase−rabbit antihuman antibodies, respectively). IgG bound to spaBC3 was removed by incubating 30 min with 50 mM sodium citrate, pH 3.0, at RT. IgG removal was validated by incubating the membrane with an appropriate secondary antibody. Immunoreactive spots were revealed using ECL Western blotting reagent (GE Healthcare).

SpaBC3-MNC Conjugation *via* Disulfide Bridges. Aliquots from a stock 2.5 M DTT solution were added to 2.8 mg of purified spaBC3 to a final concentration of 100 mM and incubated under gentle agitation for 40 min at RT. The excess of DTT was then removed by gel filtration using a prepacked PD10 column (GE Healthcare) and pre-equilibrated with 0.1 M sodium phosphate, pH 7.5, 0.1 M NaCl. Protein obtained by gel filtration (MNPA, 2.0 mg) was quantified by Bradford assay and immediately incubated at RT overnight with MNC3 (15 mg). The amount of spaBC3 bound to MNC was quantified performing a Bradford assay of supernatant. MNPA suspension (5 μL) was treated overnight with 1 M DTT. Nanoparticle content and supernatant were analyzed by dot blot.

Trastuzumab Conjugation to MNPA. The best MNPA/tz ratio to be used in the conjugation reaction was determined: MNPA containing 1 μg spaBC3 was incubated with increasing amounts of tz. After 1 h incubation, supernatants and MNPA, heated at 100 °C for 10 min in a 5× sample buffer, were loaded on SDS-PAGE performed as mentioned above. Proteins were revealed by gel code staining (Pierce Biotechnology). MNPA suspension (0.5 mL, 1 mg mL^{-1} containing 50 μg spaBC3) and PMNC (0.5 mL, 1 mg mL^{-1}) were incubated 1 h at RT with tz (150 μg). The extent of tz on the surface of MNPA and of PMNC was revealed by dot blot analysis. The amount of tz conjugated to MNPA and to PMNC was determined by difference from Bradford assay of the supernatants.

Cell Cultures. MCF-7 cells were grown in 50% Dulbecco's Modified Eagle's Medium (DMEM) and 50% F12 (EuroClone Celbio, Milan, Italy), supplemented with 10% fetal bovine serum (Hyclone Celbio, Milan, Italy), L-glutamine (2 mM), penicillin (50 UI mL^{-1}), and streptomycin (50 mg mL^{-1}, culture medium) at 37 °C in a humidified atmosphere containing 5% CO_2 and subcultured prior to confluence using trypsin/EDTA.

Immunoprecipitation Assay. MCF-7 cells were lysed with lysis buffer containing 20 mM Tris HCl, 150 mM NaCl, 10 mM EGTA, 10% glycerol, and 1% Triton X-100, pH 7.4 for 30 min at 4 °C and then centrifuged at 8500 rpm for 10 min to remove membranes and cell debris from the protein fraction. Bradford assay was used to determine protein content of whole cell extract. The preclearing step was performed with PMNC (200 μL, 1 mg mL^{-1}) for 1 h on wheel at 4 °C. The immunoprecipitation was carried out with 1 mg of precleared lysate and TMNC (200 μL, 1 mg mL^{-1}, corresponding to 3.75 μg of bound antibody) for 16 h at 4 °C on wheel. Samples were washed three times in lysis buffer and boiled in sodium dodecyl sulfate sample buffer containing 5% 2-mercaptoethanol to cleave the linkages to the beads. Samples were run on 8% polyacrylamide gel. Proteins were blotted onto PVDF membranes and incubated in blocking solution (5% skim milk in TBS, 0.05% Tween) for 1 h at RT. For HER-2 detection, membranes were then probed for 1 h at RT using anti-HER-2 polyclonal antibodies (1:500 Millipore, Billerica, MA), in blocking solution. Specificity of the interaction between the HER-2 and TMNC was verified with immunoblot of immunoprecipitated samples with unrelated proteins such as anti-Clnx pAb (1:500 Genetex), anti-Drp1 mAb (1:1000 BD transduction) both at RT for 1 h and anti-Akt pAb (1:1000 Cell Signaling, Danvers, MA) overnight in TBS + 0.05% tween +5% BSA. Specific HRP-conjugated secondary-antibodies were used always 1 h at RT (antimouse 1:10000, Bio-Rad, and antirabbit 1:2000, Cell Signaling). Immunoreactive bands were revealed using ECL Western blotting reagent (GE Healthcare).

Confocal Laser Scanning Microscopy. Cells were cultured on collagene (Sigma) precoated coverglass slides until 90% of confluence and incubated for 15 min with TMNC at a concentration of 150 μg mL^{-1} (corresponding to 15 μg of tz) or 15 μg tz in culture medium. Tz and TMNC were revealed by labeling with secondary antibodies antihuman Alexa fluor 488 (Invitrogen, Carlsbad, CA). Cultures were washed with PBS, fixed for 10 min with 4% paraformaldehyde (Sigma) and then treated for 10 min with 0.1 M glycine (Sigma) in PBS. A blocking step was performed for 1 h at RT with a solution containing 5% BSA (Sigma) and 0.1% Saponin (Sigma) in PBS, followed by 2 h incubation at RT with secondary antibody (1:300) and 30 min incubation at 37 °C with 33 μg of DiD oil (Invitrogen) in PBS for 30 min at 37 °C. Microscopy analysis was performed with a Leica SP2 AOBs microscope confocal system. Images were acquired with 63× magnification oil immersion lenses at 1024 × 1024 pixel resolution.

Acknowledgment. This paper is dedicated to Prof. Emilio Trabucchi on the occasion of his 70th birthday. We thank R. Allevi for TEM images, L. Fiandra for help in cell analyses, and E. Trabucchi for helpful discussion. This work was supported by "Fondazione Romeo ed Enrica Invernizzi" and "Centro di Microscopia Elettronica per lo sviluppo delle Nanotecnologie applicate alla medicina" (CMENA, University of Milan).

REFERENCES AND NOTES

1. Frangioni, J. V. New Technologies for Human Cancer Imaging. *J. Clin. Oncol.* **2008**, *26*, 4012–4021.
2. Weissleder, R.; Mahmood, U. Molecular Imaging. *Radiology* **2001**, *219*, 316–333.
3. Kim, E. E. *Molecular and Cellular MR Imaging.*; Modo, M. M. J., Bulte, J. W. M., Eds.; CRC Press: Boca Raton, FL, 2007; pp 1−421.
4. Caravan, P.; Ellison, J. J.; McMurry, T. J.; Lauffer, R. B. Gadolinium(III) Chelates as MRI Contrast Agents: Structure, Dynamics, and Applications. *Chem. Rev.* **1999**, *99*, 2293.

5. Terreno, E.; Delli Castelli, D.; Viale, A.; Aime, S. Challenges for Molecular Magnetic Resonance Imaging. *Chem. Rev.* **2010**, *110*, 3019–3042.
6. Konda, S. D.; Aref, M.; Brechbiel, M.; Wiener, E. C. Development of a Tumor-Targeting MR Contrast Agent using the High-Affinity Folate Receptor-Work in Progress. *Invest. Radiol.* **2000**, *35*, 50–57.
7. Ke, T.; Jeong, E.-K.; Wang, X.; Feng, Y.; Parker, D. L.; Lu, Z.-R. RGD Targeted Poly(L-glutamic acid)-cystamine-(Gd-DO3A) Conjugate for Detecting Angiogenesis Biomarker Anb3 Integrin with MR T_1 Mapping. *Int. J. Nanomed.* **2007**, *2*, 191–199.
8. Curtet, C.; Tellier, C.; Bohy, J.; Conti, M. L.; Saccavini, J. C.; Thedrez, P.; Douillard, J. Y.; Chatal, J. F.; Koprowski, H. Selective Modification of NMR Relaxation Time in Human Colorectal Carcinoma by Using Gadolinium-diethylenetriaminepentaacetic Acid Conjugated with Monoclonal Antibody 19-9. *Proc. Natl. Acad. Sci. U.S.A.* **1986**, *83*, 4277–4281.
9. Morawski, A. M.; Winter, P. M.; Crowder, K. C.; Caruthers, S. D.; Fuhrhop, R. W.; Scott, M. J.; Robertson, J. D.; Abendschein, D. R.; Lanza, G. M.; Wickline, S. A. Targeted Nanoparticles for Quantitative Imaging of Sparse Molecular Epitopes with MRI. *Magn. Reson. Med.* **2004**, *51*, 480–486.
10. Mendonca Dias, M. H.; Lauterbur, P. C. Ferromagnetic Particles as Contrast Agents for Magnetic Resonance Imaging of Liver and Spleen. *Magn. Reson. Med.* **1986**, *3*, 328–330.
11. Semelka, R. C.; Helmberger, T. K. Contrast Agents for MR Imaging of the Liver. *Radiology* **2001**, *218*, 27–38.
12. Harisinghani, M. G.; Barentsz, J.; Hahn, P. F.; Deserno, W. M.; Tabatabaei, S.; van de Kaa, C. H.; de la Rosette, J.; Weissleder, R. Noninvasive Detection of Clinically Occult Lymph-Node Metastases in Prostate Cancer. *N. Engl. J. Med.* **2003**, *348*, 2491–2499.
13. de Vries, I. J. M.; Lesterhuis, W. J.; Barentsz, J. O.; Verdijk, P.; van Krieken, J. H.; Boerman, O. C.; Oyen, W. J. G.; Bonenkamp, J. J.; Boezeman, J. B.; Adema, G. J.; *et al*. Magnetic Resonance Tracking of Dendritic Cells in Melanoma Patients for Monitoring of Cellular Therapy. *Nat. Biotechnol.* **2005**, *23*, 1407–1413.
14. Evgenov, N. V.; Medarova, Z.; Dai, G.; Bonner-Weir, S.; Moore, A. *In Vivo* Imaging of Islet Transplantation. *Nat. Med.* **2006**, *12*, 144–148.
15. Perez, J. M.; Josephson, L.; O'Loughlin, T.; Hogemann, D.; Weissleder, R. Magnetic Relaxation Switches Capable of Sensing Molecular Interactions. *Nat. Biotechnol.* **2002**, *20*, 816–820.
16. Shultz, M. D.; Reveles, J. U.; Khanna, S. N.; Carpenter, E. E. Reactive Nature of Dopamine as a Surface Functionalization Agent in Iron Oxide Nanoparticles. *J. Am. Chem. Soc.* **2007**, *129*, 2482–2487.
17. Narain, R.; Gonzales, M.; Hoffman, A. S.; Stayton, P. S.; Krishnan, K. M. Synthesis of Monodisperse Biotinylated p(NIPAAm)-Coated Iron Oxide Magnetic Nanoparticles and Their Bioconjugation to Streptavidin. *Langmuir* **2007**, *23*, 6299–6304.
18. Polito, L.; Monti, D.; Caneva, E.; Delnevo, E.; Russo, G.; Prosperi, D. One-Step Bioengineering of Magnetic Nanoparticles *via* a Surface Diazo Transfer/Azide−Alkyne Click Reaction Sequence. *Chem. Commun.* **2008**, *5*, 621–623.
19. Polito, L.; Colombo, M.; Monti, D.; Melato, S.; Caneva, E.; Prosperi, D. Resolving the Structure of Ligands Bound to the Surface of Superparamagnetic Iron Oxide Nanoparticles by High-Resolution Magic-Angle Spinning NMR Spectroscopy. *J. Am. Chem. Soc.* **2008**, *130*, 12712–12724.
20. Hober, S.; Nord, K.; Linhult, M. Protein A Chromatography for Antibody Purification. *J. Chromatogr., B* **2007**, *848*, 40–47.
21. Abrahmsen, L.; Moks, T.; Nilsson, B.; Hellmann, U.; Uhlèn, M. Analysis of Signal for Secretion of *Staphylococcal* Protein A Gene. *EMBO J.* **1985**, *13B*, 3901–3906.
22. Chalon, M. P.; Milne, R. W.; Vaerman, J. P. Interactions between Mouse Immunoglobulins and *Staphylococcal* Protein A. *Scand. J. Immunol.* **1979**, *9*, 359–364.
23. Holschuh, A.; Schwammle, J. Preparative Purification of Antibodies with Protein A—An Alternative to Conventional Chromatography. *J. Magn. Magn. Mater.* **2003**, *293*, 345–348.
24. Hoffman, W. L.; O'Shannessy, D. J. Site-Specific Immobilization of Antibodies by their Oligosaccharide Moieties to New Hydrazide Derivatized Solid Supports. *J. Immunol. Methods* **1998**, *112*, 113–120.
25. Colombo, M.; Corsi, F.; Foschi, D.; Mazzantini, E.; Mazzucchelli, S.; Morasso, C.; Occhipinti, E.; Polito, L.; Prosperi, D.; Ronchi, S.; *et al*. HER2 Targeting as a Two-Sided Strategy for Breast Cancer Diagnosis and Treatment: Outlook and Recent Implications in Nanomedical Approaches. *Pharmacol. Res.* **2010**, *62*, 150–165.
26. Park, J.; An, K.; Hwang, Y.; Park, J.-G.; Noh, H.-J.; Kim, J.-Y.; Park, J.-H.; Hwang, N.-M.; Hyeon, T. Ultra-large-Scale Syntheses of Monodisperse Nanocrystals. *Nat. Mater.* **2004**, *3*, 891–895.
27. See, for example: Ma, H.-l.; Qi, Xi.-r.; Maitani, Y.; Nagai, T. Preparation and Characterization of Superparamagnetic Iron Oxide Nanoparticles Stabilized by Alginate. *Int. J. Pharm.* **2007**, *333*, 177–186.
28. Halling, P. J.; Dunnill, P. Hydrolysis of Lactose in Milk by Lactase Immobilized to a Non-porous magnetic Support. *Appl. Microbiol. Biotechnol.* **1979**, *8*, 27–36.
29. De Marco, V.; Stier, G.; Blandin, S.; De Marco, A. The Solubility and Stability of Recombinant Proteins are Increased by their Fusion to NusA. *Biochem. Biophys. Res. Commun.* **2004**, *322*, 766–771.
30. Carlsson, J.; Drevin, H.; Axèn, R. Protein Thiolation and Reversible Protein−Protein Conjugation. *Biochem. J.* **1978**, *173*, 727–730.
31. Stuchbury, T.; Shipton, M.; Norris, R.; Malthouse, P. J.; Brocklehurst, K. A; Herbert, J. A. L.; Suschitzky, H. Reported Group Delivery System with Both Absolute and Selective Specificity for Thiol Groups and an Improved Fluorescent Probe Containing the 7-Nitrobenzo-2-oxa-1,3-diazole Moiety. *Biochem. J.* **1975**, *151*, 417–432.
32. Corsi, F.; De Palma, C.; Colombo, M.; Nebuloni, M.; Ronchi, S.; Rizzi, G.; Allevi, R.; Tosoni, A.; Trabucchi, E.; Clementi, E.; Prosperi, D. Towards Ideal Magnetofluorescent Nanoparticles for Bimodal Detection of Breast Cancer Cells. *Small* **2009**, *5*, 2555–2564.
33. Yuste, L.; Montero, J. C.; Espari's-Ogando, A.; Pandiella, A. Activation of ErbB2 by Overexpression or by Transmembrane Neuregulin Results in Differential Signaling and Sensitivity to Herceptin. *Cancer Res.* **2005**, *65*, 6801–6810.
34. Navath, R. S.; Kurtoglu, Y. E.; Wang, B.; Kannah, S.; Romero, R.; Kannan, R. M. Dendrimer−Drug Conjugates for Tailored Intracellular Drug Release Based on Glutathione Levels. *Bioconjugate Chem.* **2008**, *19*, 2446–2455.
35. Sambrook, J.; Fritsch, E. F.; Maniatis, T. In *Molecular Cloning: A Laboratory Manual*, 2nd ed.; Nolan, C., Ed.; Cold Spring Harbor Laboratory Press: Cold Spring Harbor, NY, 1989; Vol. 1.
36. Laemmli, U. K. Cleavage of Structural Proteins During the Assembly of the Head of Bacteriophage T4. *Nature* **1970**, *227*, 680–685.